ENERGY HARVESTING FROM A NONLINEAR PIEZOELECTRIC OSCILLATOR SUBJECTED TO RANDOM AND HARMONIC EXCITATIONS

Tiago Leite Pereira, tiagolei.tl@gmail.com
Aline Souza de Paula, alinedepaula@unb.br
Adriano Todorovic Fabro, fabro@unb.br
Universidade de Brasília, Department of Mechanical Engineering
70.910.900 - Brasília – DF, Brazil

Marcelo Amorim Savi, savi@ufrj.br
Universidade Federal do Rio de Janeiro, COPPE , Department of Mechanical Engineering
21.941.972 – Rio de Janeiro – RJ, Brazil, P.O. Box 68.503

Abstract. *Many alternative energy sources have been investigated in the last decades, energy harvesting from the environment is of these possibilities and have been explored recently by using piezoelectric material. This vibration-based energy harvesting using piezoelectric elements is possible by exploring the direct effect, where the piezoelectric material is able convert mechanical in to electrical energy, and can be very useful for applications in powering small electronic devices. Analyses involving oscillators subjected to harmonic excitations have been well studied, demonstrating that nonlinearities can enhance the harvested energy, mostly the nonlinearities that lead to bistable oscillators. This work addresses the influence of nonlinearities in energy harvesting from a piezomagnetoelastic structure subjected to random and harmonic vibrations. The energy harvesting system is a magnetoelastic structure that consists of a ferromagnetic cantilevered beam with two permanent magnets, one located in the free end of the beam and the other at a vertical distance* ***d*** *from the beam free end, subjected to harmonic and random base excitation. In order to use this device as a piezoelectric power generator, two piezoceramic layers are attached to the root of the cantilever and a bimorph generator is obtained. Nonlinear equations of motion that describe the electromechanical system are given along with theoretical simulations. The numerical analysis presents a comparison between the average electrical power provided from nonlinear system and the Power Spectral Density (PSD) of the electrical power due to two different excitations, at first a harmonic excitation after random excitation. The goal of the proposed analysis is to establish how the average electrical power and PSD value evaluated the system.*

Keywords: *Energy harvesting, Piezoelectric Material, Random excitation, nonlinear system.*

1 INTRODUCTION

Energy harvesting is a process able to convert the available energy in the environment in electrical energy. There are many source of vibration energy, using piezoelectric material the mechanical energy available in the ambient can be harvested in electrical energy by the direct effect and this energy can be used or stored. Recent works present the significant contribution of the researches in energy harvesting (Anton and Sodano, 2007), (Tang et al., 2010). In linear systems the best energy harvesting performance is achieved when the system is excited at its resonance frequency, if the excitation slightly change the electrical response of the systems is reduced. Nonlinearities allow a broadband, some works show that nonlinearities can enhance the harvested energy (Shahruz, 2007), (Ramlan et al., 2009). In a recent work (Erturk et al., 2009), considering a harmonic excitation, was showed that the broadband behavior can be obtained by exploring nonlinearities of a bistable piezomagnetoelastic. Lefeuvre (Lefeuvre et al., 2007) were one of the first to investigate an energy harvesting system subjected to a random excitation. The system was also studied by Kumar (Kumar et al., 2014), a Gaussian white noise was considered, and an investigation of the effects of the system parameters on the mean square voltage was studied. De Paula (De Paula et al., 2015) presented a numerically and experimentally investigation of the piezomagnetoelastic system when it is subjected to a Gaussian white noise and presented the influence of nonlinearities in the system. A comparison between the voltage provided from a linear, nonlinear bistable and nonlinear monostable systems was also investigated for De Paula, showing that for a bistable system the better RMS voltage is when the system visit both stable point. Therefore, this paper presents a numerical analysis aiming to compare the average power produced and its efficiency from the given non-linear system and its PSD for two different types of excitation, firstly a harmonic and then a random white noise excitation. In section 1, a general introduction and general overview is presented. Section 2 presents the piezomagnetoelastic system and the main features of its dynamic behavior. Section 3 shows some numerical results and discussion considering harmonic and random white noise excitation. Finally, in Section 4 some conclusion and final remarks are drawn.

2 HARVESTING ENERGY FROM A NON LINEAR PIEZOMAGNETOELASTIC STRUCTURE

2.1 The piezomagnetoelastic system

The energy harvesting system is based on a magnetoelastic structure first investigated by Moon and Holmes (Moon and Holmes, 1979), and consists of a ferromagnetic cantilevered beam with two permanent magnets, one located in the free end of the beam and the other at a vertical distance *d* from the beam free end, subjected to harmonic and random base excitation. In order to use this device as a piezoelectric power generator, two piezoceramic layers are attached to the root of the cantilever and a bimorph generator is obtained.

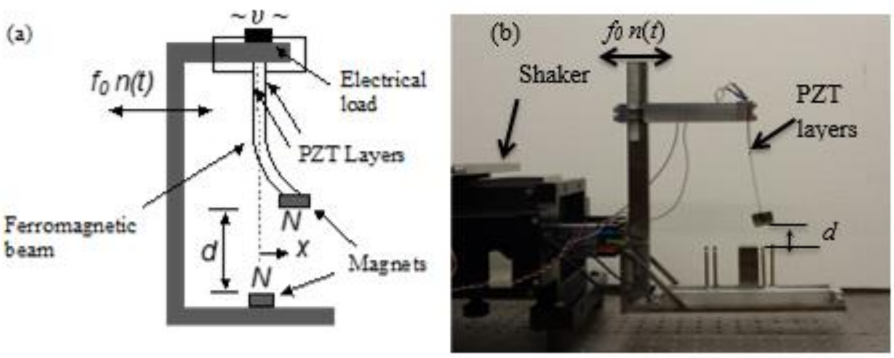

Figure 1. (a) Schematic representation of the piezomagnetoelastic structure and (b) picture of the actual structure.

The system presented in Figure 1 is governed by equations (1) and (2)

$$\ddot{x} + 2\zeta\dot{x} - \frac{1}{2}x(1 - x^2) - \chi v = F(t), \quad (1)$$

$$\dot{v} + \lambda v + \kappa\dot{x} = 0\,, \quad (2)$$

where x is the dimensionless tip displacement of the beam in the transverse direction, v is the dimensionless voltage across the load resistence. The constant ζ is the mechanical damping ratio, χ is the dimensionless piezoelectric coupling term in the mechanical equation, κ is the dimensionless piezoelectric coupling term in the electrical circuit equation, and λ is the reciprocal of the dimensionless time constant ($\lambda \propto 1/R_L C_P$ where R_L is the load resistance and C_P is the equivalent capacitance of the piezoceramic layers). $F(t)$ is the forcing of the system, for a harmonic excitation $F(t) = f_0 cos(\omega t)$, where f_0 is the dimensionless excitation due to base acceleration ($f \propto \Omega^2 X_0$ where X_0 is the dimensionless base displacement amplitude). And for a random excitation $F(t) = f\ N(t)$, where f is the dimensionless magnitude of excitation and forcing function $N(t)$ is a Gaussian white noise. The values of the parameters are considered as the same as in Erturk (Erturk et al., 2009), ζ = 0.01, χ = 0.05, κ=0.5, λ=0.05. By considering these parameters, the equilibrium points, that can be obtained from Eq. (1) and (2), are two stable spiral points located at $(x , \dot{x} ,v)=(\pm 1,0,0)$ and one instable saddle point located at $(x , \dot{x} , v)=(0,0,0)$.

The instantaneous dimensionless mechanical power is given by,

$$P_{mec}^{i} = F(t)\dot{x}(t), \quad (3)$$

where $F(t)$ is the excitation force and the superscript i stands for instantaneous value of the Power.

The dimensionless electrical power harvested by the piezomagnetoelastic structure is defined by

$$P_{ele}^{i} = iv, \quad (4)$$

where the $i = \lambda v$ is the dimensionless current.

Moreover, the average value of the effective instantaneous power is given by

$$P^m = \frac{1}{t}\sqrt{\int_0^t (P^i)^2}\ dt\ . \tag{5}$$

the subscript *m* stands for the average value of the Power.

The system can be evaluated by its efficiency, defined by the ratio of the dimensionless average electrical power P^m_{ele} and the dimensionless average mechanical power P^i_{mec}, i.e.

$$\eta = \frac{P^m_{ele}}{P^m_{mec}}\ . \tag{6}$$

The system can be also evaluated in terms of the Power Spectral Density (PSD) (Newland, 2005) by

$$r = \frac{\int_0^\omega PSD_{out}(\omega)d\omega}{\int_0^\omega PSD_{in}(\omega)d\omega}\ . \tag{7}$$

where PSD_{in} is the value of *PSD* from *F(t),* and PSD_{out} is calculated from χv that is a dimensionally corresponding term to *F(t)*. The PSD is calculated for both a periodic and random excitation using a periodogram approach and Hanning windowing.

2.2. Dynamic Behavior

At first, harmonic excitation is of concern. Figure 2 shows the qualitative change of system response from bifurcation diagrams by varying forcing parameters. In both diagrams, Figure 2 (a) and (b), black point considers the system starting at $\omega = 0.8$ and $f_0 = 0.083$ with initial conditions $(x, \dot{x}, v) = (1,0,0)$ which correspond to a chaotic response. Note that this behavior consists in a region in the middle of the bifurcation diagrams. From this chaotic response two analyses are evaluated. In Figure 2 (a), value of f_0 is increased and decreased and plotted together in the diagram. While in Figure 2 (b), value of ω is increased and decreased and once again plotted together in the bifurcation diagram. From this analysis, the diagrams indicate periodic and chaotic behaviors. The pink point presents a similar analysis, however, the system is started at $\omega = 0.8$ and $f_0 = 0.083$ with initial condition $(x, \dot{x}, v) = (1,1,0)$ which correspond to periodic orbit of periodicity 1. From this analysis, only periodic behavior is observed. By considering black and pink points of both bifurcation diagrams, coexisting attractors are observed. In the following analysis, some of these responses are investigated.

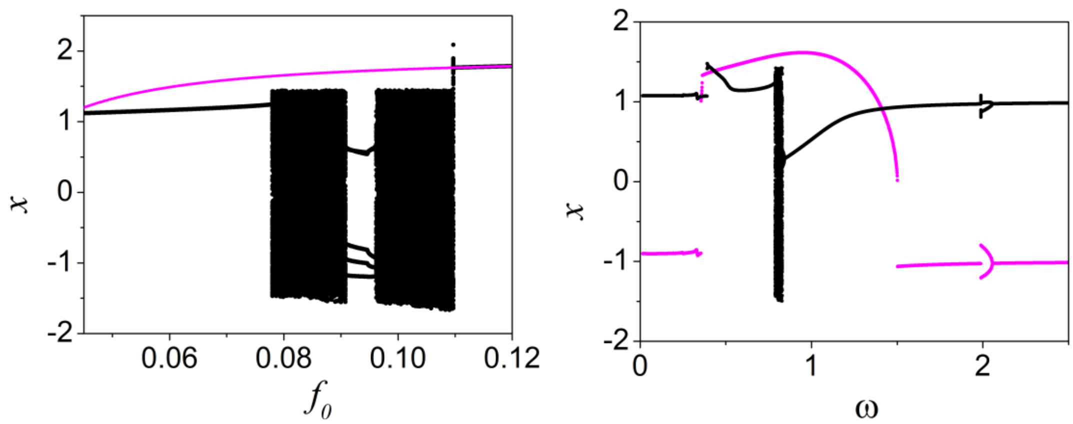

Figure 2. Bifurcation Diagram, (a) ranging the amplitude f_0 and ω fixed in 0.8 (b) and ranging the frequency ω and f_0 fixed in 0.083.

For a better understanding of the behavior of the system, Figure 3 (a) presents the response in time domain of the tip displacement obtained at ω = 0.8 and f_0= 0.083 with initial condition $(x, \dot{x}, v) = (1,1,0)$, and Figure 3 (b) shows the phase space and Poincaré section which correspond to a periodic response. While Figure 4 shows a response for the same forcing parameters and initial conditions $(x, \dot{x}, v) = (1,0,0)$. Figure 4 present (a) the tip displacement, (b) the phase space and (c) the Poincaré Section.

From the bifurcation diagram presented in Figure 2, different responses of the system can be seen. For proposed the analysis, 8 different cases of the response of the system, based on their position at the bifurcation diagram, are used. Cases 1 to 4 are part of the bifurcation diagram with varying ω and Cases 5 to 8 are part of the bifurcation diagram with varying f_0. Figure 5 shows the phase space and Poincaré section for such cases. Note that the phase space and Poincaré section of Cases 2 and 3 are at Figure 3 and 4, respectively. Cases 3 and 7 represent chaotic responses and Cases 1, 2, 4, 5, 6 and 8 represent periodic responses. Table 1 present the forcing parameters along with the respective initial conditions for each case.

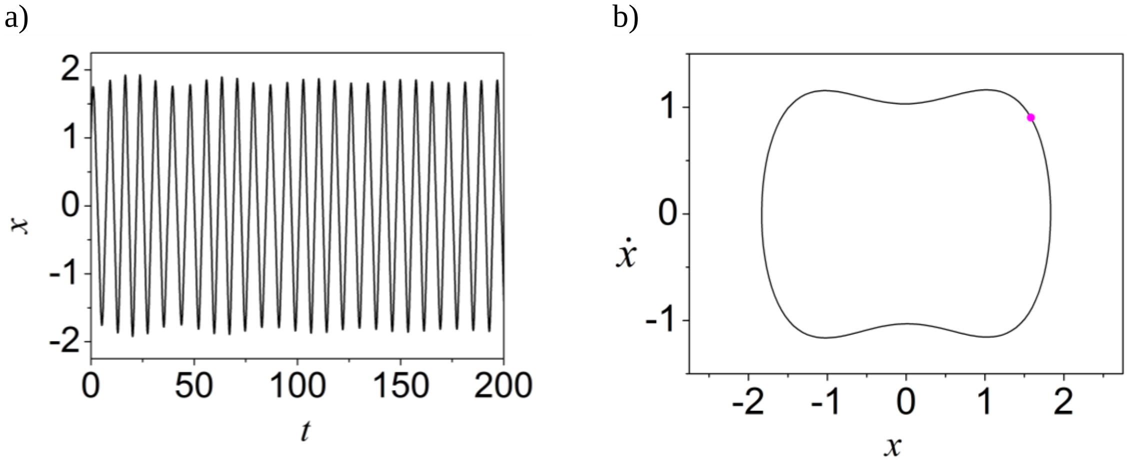

Figure 3. (a) Tip displacement of the system in time domain with f_0=0.083 and ω = 0.8 and initial conditions $(x, \dot{x}, v) = (1,1,0)$, and its (b) phase space and Poincaré section.

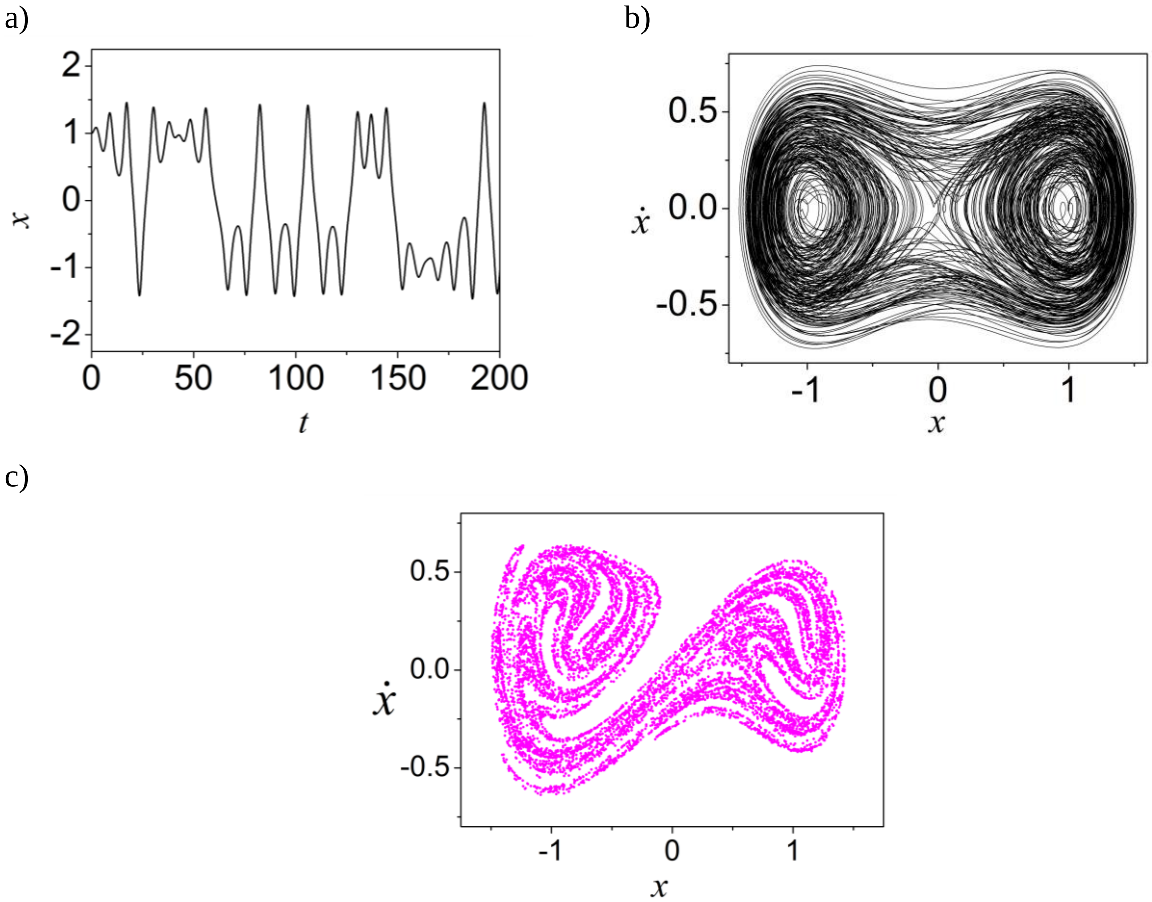

Figure 4 (a) Tip displacement of the system in time domain with f_0=0.083 and ω = 0.8 and initial conditions (x , $\dot{x}$, v) = (*1,0,0*) , and its (b) phase space and (c) Poincaré section.

Table 1. Forcing parameters and initial conditions for each of the considered cases.

	ω	f_0	Initial Condition	Behavior
Case 1	0.5	0.083	*(1.4263,0.4801,-0.7263)*	*Periodic*
Case 2	0.8	0.083	*(1,1,0)*	*Periodic*
Case 3	0.8	0.083	*(1,0,0)*	*Chaotic*
Case 4	1.4	0.083	*(0.9609, 2.966, -0.5192)*	*Periodic*
Case 5	0.8	0.031	(*0.1765, 1.0371, 0.0090*)	*Periodic*
Case 6	0.8	0.07	(*1.4895, 0.9918, -0.7675*	*Periodic*
Case 7	0.8	0.1	(*-1.2316,-0.0048, 0.3478*)	*Chaotic*
Case 8	0.8	0.15	(*1.7766, 0.6094,-0.8985*)	*Periodic*

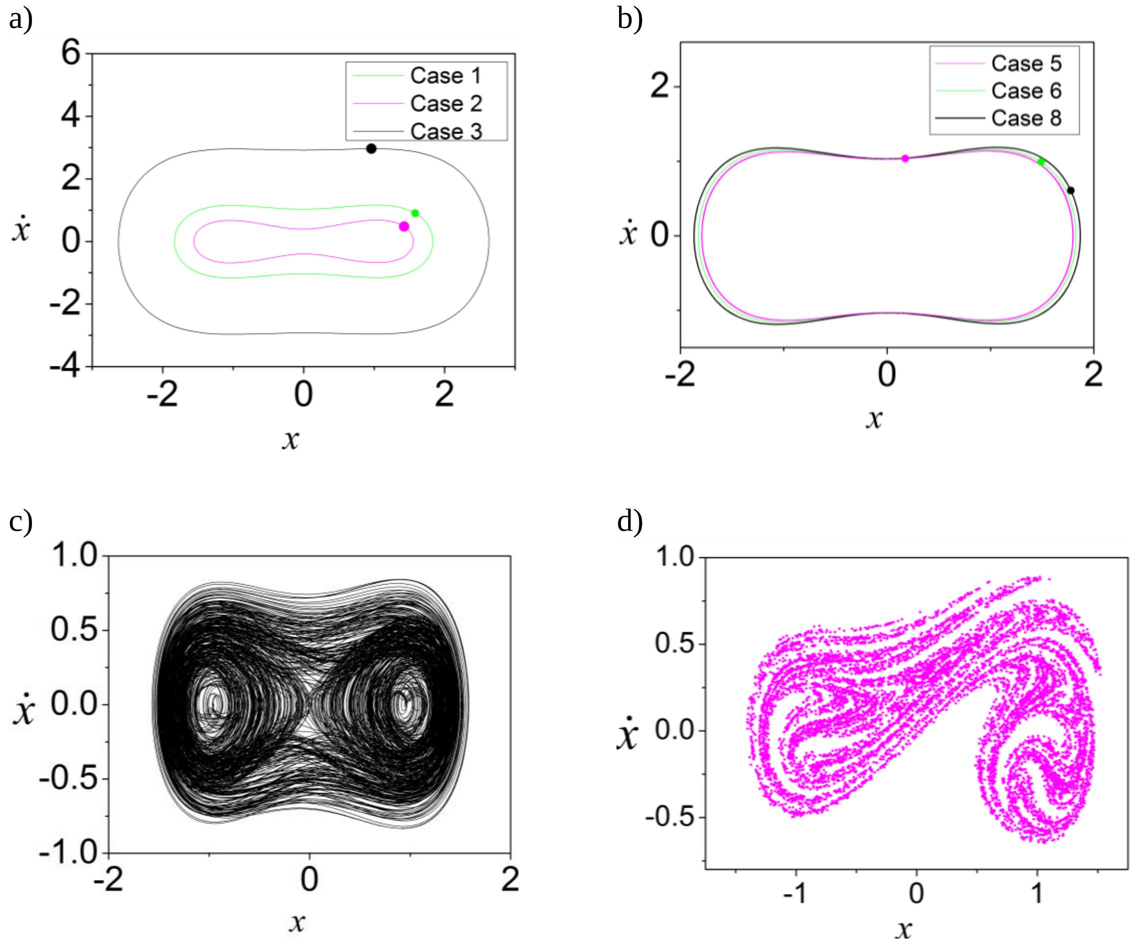

Figure 5. The phase space and poincaré section for Cases 1 to 8.

3 NUMERICAL RESULTS AND DISCUSSION

In this section, numerical simulations are presented for both harmonic only and random white noise only forcing. Firstly, the value of the input electrical power and the mechanical power of the tip displacement of the beam to the harmonic excitation only are presented. Therefore, the value of the efficiency presented here is the efficiency of the piezoelectric material. Also the *PSD* of the electrical output χv and of the tip displacement $x/2$ is calculated. Secondly, an analogous analysis is presented but with a random with noise only forcing. Results with harmonic and random white noise forcing applied at the same time are not presented in this analysis.

3.1 Harmonic excitation

The dimensionless electrical and mechanical powers, Eq. (3) and (4), are evaluated for the periodic response presented in Fig. 3, and results are shown in Fig. 6. After 100 forcing periods, the obtained average dimensionless electrical power is 0.0176 (Fig. 6a) and the average dimensionless mechanical power is 0.0461 (Fig. 6b), leading to an efficiency of 38.45%. Figure 7 presents the results obtained for the chaotic behavior, identified in Fig. 4. In this case, the obtained average dimensionless electrical power after 100 forcing periods is

0.0073 (Fig. 7a) and the average dimensionless mechanical power is 0.0132 (Fig. 7b), leading to an efficiency of 55.55%. Comparing both periodic and chaotic behavior, it can be noted that the periodic case shows a higher dimensionless electrical average power but the chaotic has a better efficiency.

a) b)

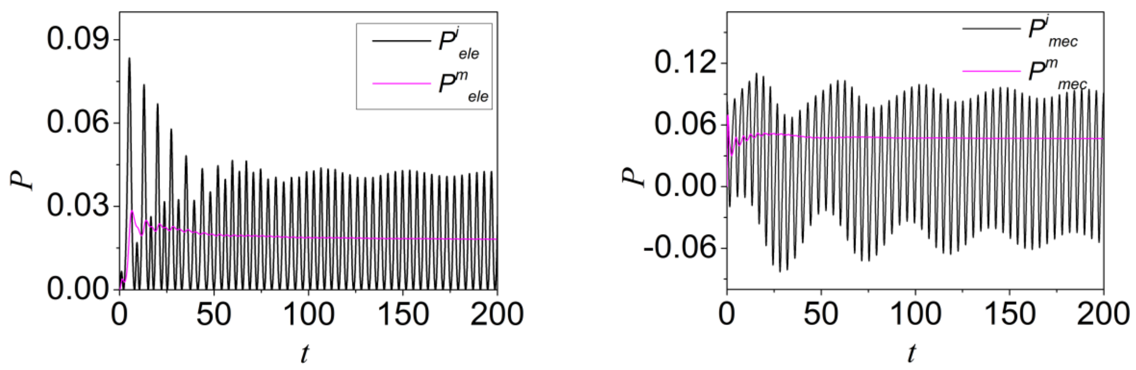

Figure 6. (a) Electrical Power and (b) mechanical power for f_0=0.083, ω = 0.8 and initial conditions (*1,1,0*)

a) b)

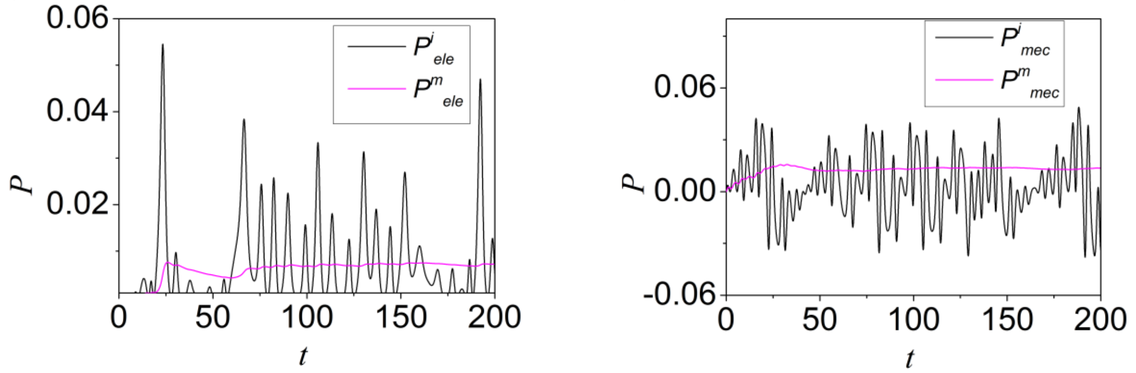

Figure 7. (a) Electrical Power and (b) mechanical power for f_0=0.083, ω = 0.8 and initial conditions (*1,0,0*)

Figures 8 and Figure 9 present the results obtained with the system response as identified in Figure 2, after 100 forcing periods, in terms of not only the dimensionless average electrical and mechanical powers but also the efficiency is plotted. The black points are referred to the systems starting at $\omega = 0.8$ and $f_0 = 0.083$ with initial conditions $(x, \dot{x}, v) = (1,0,0)$, which correspond to a chaotic response, and the pink points present a similar analysis, but with the system starting at $\omega = 0.8$ and $f_0 = 0.083$ with initial conditions $(x, \dot{x}, v) = (1,1,0)$, which correspond to a periodic orbit of periodicity 1. In Figure 8 (a), the value of f_0 is increased and decreased and results are plotted together. Similarly, in Figure 9, the value of ω is increased and decreased and results are plotted together.

It can be observed from the pink points in Figure 8 that the value of the efficiency is decreasing according with the increasing of the value of f_0. Although the value of electrical power remains constant, Figure 8 (a), the value of mechanical power increases, Figure 8 (b), decreasing the value of efficiency, Figure 8 (c).

The system can be also evaluated by the values of ratio of *PSD,* Eq. (7). For the output value, the term χv is used so that it has the same dimension of the input force *F(t)*. For input force we use the value $f_0cos(\omega t)$. Figure 10 shows the *PSD* for the cases of (a) periodic response, case 2, and (b) chaotic response, case 3.

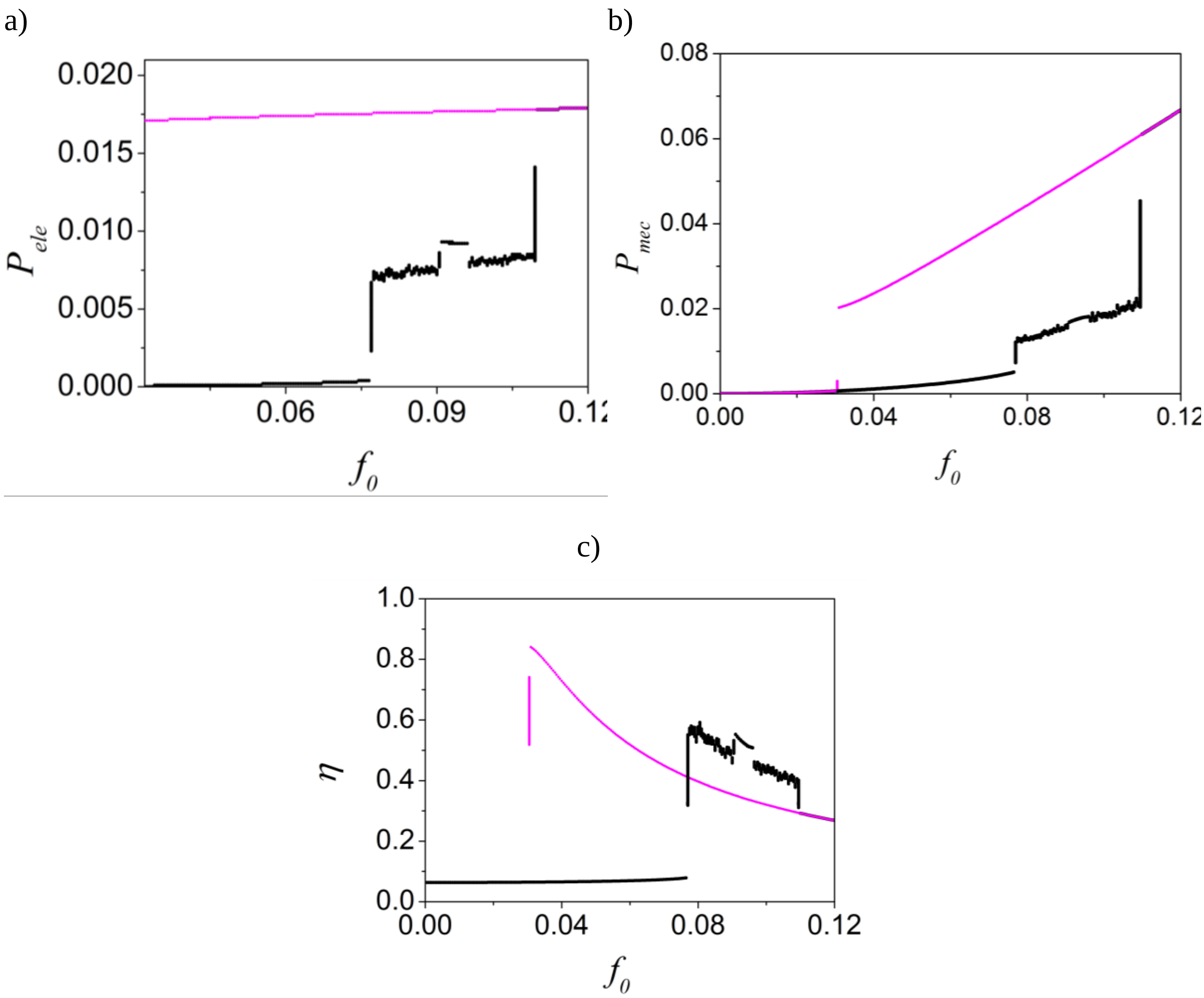

Figure 8. The dimensionless (a) electrical and (b) mechanical powers and (c) the given efficiency for initial conditions leading to (black) chaotic behavior and (pink) periodic orbit of periodicity and ranging the values of f_0 and ω fixed in 0.8 (black).

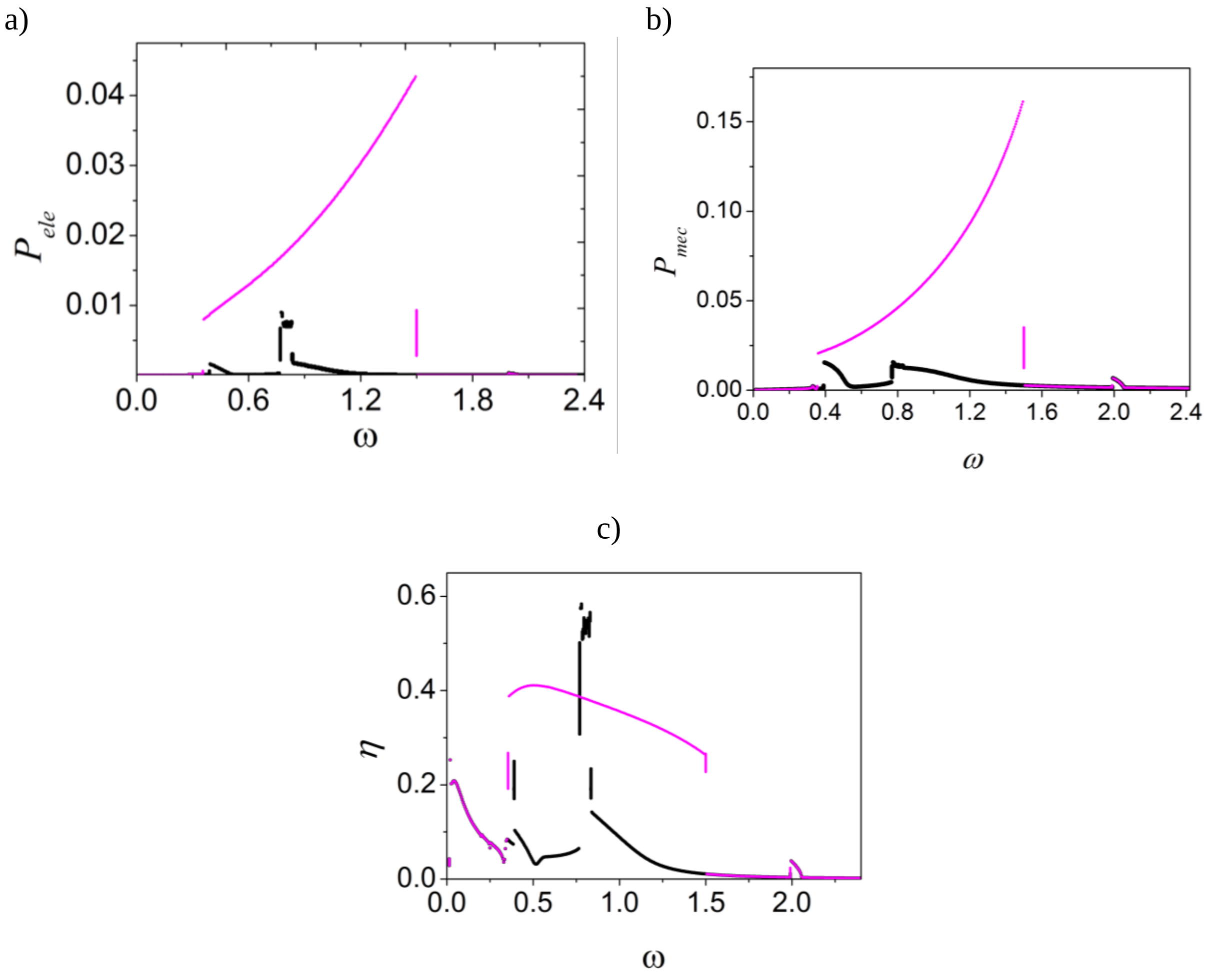

Figure 9. The dimensionless (a) electrical and (b) mechanical powers and (c) the given efficiency for initial conditions leading to (black) chaotic behavior and (pink) periodic orbit of periodicity and ranging the values of ω and fixed f_0 in 0. 083

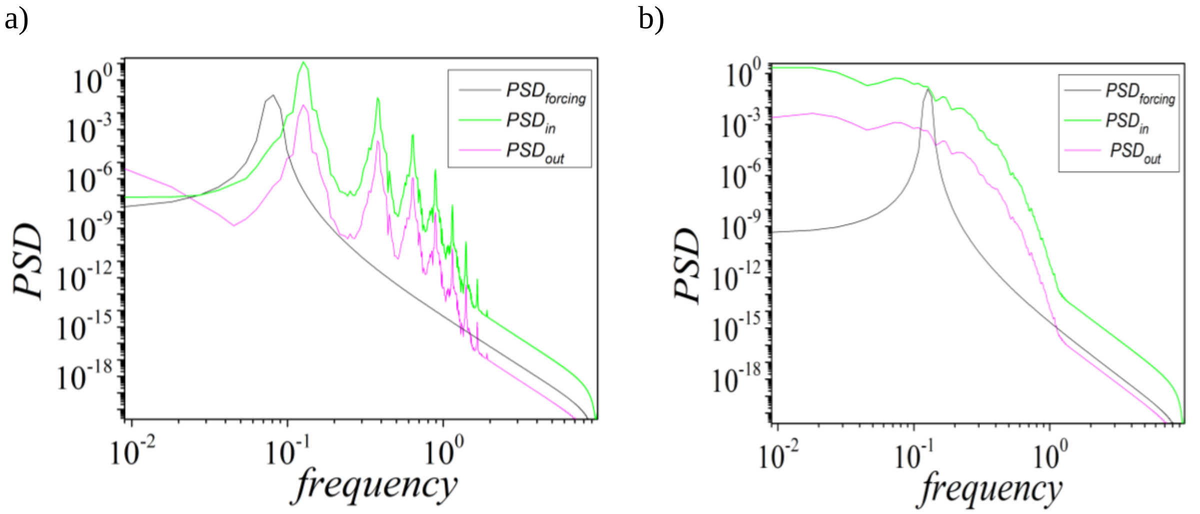

Figure 10. PSD for two orbits for f_0=0.083 and ω = 0.8 with initial condition (a) *(1, 1, 0)*, periodic, and *(b) (1, 0, 0)*, chaotic.

Two different approaches are used for the analysis of all of the considered cases. The first approach uses the value of efficiency, as defined in Eq. (6), relating the values of the electrical P_{ele}^{m} and mechanical P_{mec}^{m} powers. The former, refers to the average effective electrical power harvested by the piezoelectric material, Eq. (4), and the latter, refers to the average effective mechanical power of the tip displacement of the beam after 100 forcing periods, Eq. (3).

In the second approach, the ratio of the PSD, is defined from Eq. (7) from the input value, i.e. he tip displacement of the beam $x/2$, and from the output value, i.e. χv, Eq. (1). Therefore, P_{mec}^{m} and PSD_{in} are related to the input value of the tip displacement and P_{ele}^{m} and PSD_{out} are related to the output voltage, so η is the ratio of the average electrical power to the average mechanical power, i.e. efficiency of the piezoelectric material. And the value of r is the ratio of PSD_{out} for PSD_{in}.

Table 2 present the results obtained from the first approach and comparing the best piezoelectric performance using the efficiency of the piezoelectric material. It can be observed that Case 3, chaotic response, presents the high efficiency, or piezoelectric performance, nevertheless the lowest value of electrical power, while Case 4, periodic response, presents a much lower value of efficiency despite having the biggest value of electrical power. It can be also observed that Case 5 presents the best efficiency of Table 2.

The results obtained from the second approach are presented in Table 3. It can be observed that the best electrical output is for the Case 8. Cases 5, 6 and 8 presents the same efficiency, although the PSD_{out} and PSD_{in} have different values for each case. The lowest value for the efficiency and PSD_{out} are present for Case 3, which is a chaotic behavior. According with the PSD_{out} the best case of the system is Case 4, and the lowest value of the PSD_{out}, case 3.

Table 2. Efficiency, mechanical and electrical powers obtained with harmonic excitation, Cases 1 to 8.

		Case 1	Case 2	Case 3	Case 4
f_0 \ ω		0.5 Periodic	0.8 Periodic	0.8 Chaotic	1.4 Periodic
0.083	η	41.09%	38.29%	53.01%	28.77%
	P^{m}_{mec}	0.0264	0.04600	0.0137	0.1336
	P^{m}_{ele}	0.0108	0.0176	0.0072	0.0384
		Case 5	Case 6	Case 7	Case 8
ω \ f_0		0.031 Periodic	0.07 Periodic	0.1 Chaotic	0.15 Periodic
0.8	η	84.01%	44.96%	44.17%	21.55%
	P_{mec}^{m}	0.0202	0.0388	0.0180	0.0841
	P_{ele}^{m}	0.0170	0.0174	0.0079	0.0181

Table 3. PSD input, output and ratio *r* obtained with harmonic excitation, Cases 1 to 8.

		Case 1	Case 2	Case 3	Case 4
f_0 \ ω		0.5 Periodic	0.8 Periodic	0.8 Chaotic	1.4 Periodic
0.083	r	0.2475%	0.2490%	0.1861%	0.2497%
	PSD_{in}	38.9315	39.1621	21.3987	48.7676
	PSD_{out}	0.0963	0.0975	0.0398	0.1217
		Case 5	Case 6	Case 7	Case 8
ω \ f_0		0.031 Periodic	0.07 Periodic	0.1 Chaotic	0.15 Periodic
0.8	r	0.2490%	0.2490%	0.2106%	0.2490%
	PSD_{in}	54.1096	55.5721	30.2220	57.6053
	PSD_{out}	0.1347	0.1383	0.0636	0.1434

3.2 Random white noise excitation

In this section, the forcing term is given by $f_0N(t)$, where $N(t)$is a zero-mean random Gaussian white noise stochastic process with variance σ^2. The analysis follows the same approaches than for the harmonic excitation, i.e. the average electrical and mechanical powers of the output voltage and beam tip displacement, respectively, as well as the efficiency of the piezoelectric material. Also, the PSD_{out}, PSD_{in} and r are calculated.

Figure 11 (a) shows the tip displacement of the beam in time domain. The oscillation between the two stable points can be clearly noted. Figure 11 (b) presents the electrical power and it can be observed that the higher instantaneous electrical power occurs when the system visit both stable points, which agrees with the results obtained by De Paula et al (De Paula et al., 2015). In Figure 2 it can be observed that the highest value of PSD are presented for low frequencies, and it doesn't present a peak as presented in a periodic response in a harmonic excitation.

Three different values of the forcing parameter f_0 are chosen and for each one $N(t)$ is simulated with four different values of σ^2, in a total of twelve cases named from Case 9 to Case 20. For all cases, the initial conditions are given by (x , $\dot{x}$, v) = ($0,0,0$), i.e. the unstable equilibrium point.

Tables 4 and 5 present the obtained results for the first and second approaches, respectively, as described in the previous section. From Table 4, it can be observed that for all cases, for an increasing σ^2 the values of mechanical and electrical powers are also increasing. For an increasing σ^2 , the values of the efficiency η also increase for cases 9 to 12, but they decrease for cases 13 to 20. From Table 5, it can be observed that for all cases, for an increasing σ^2 the values of PSD_{out} are also increasing. However for an increasing σ^2 the value of PSD_{in} are decreasing for Cases 9 to 12, and increasing for Cases 17 to 20, in Cases 13 to 16 the PSD_{in} are increasing but Case 14 does not obey this pattern.

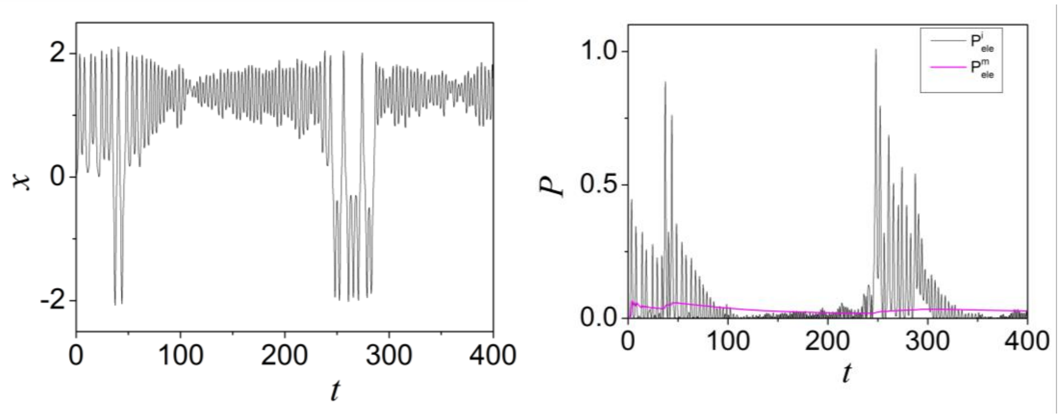

Figure 11. (a) Tip displacement and the (b) electrical power in time domain for $\sigma^2 = 1$ and $f_0 = 1$.

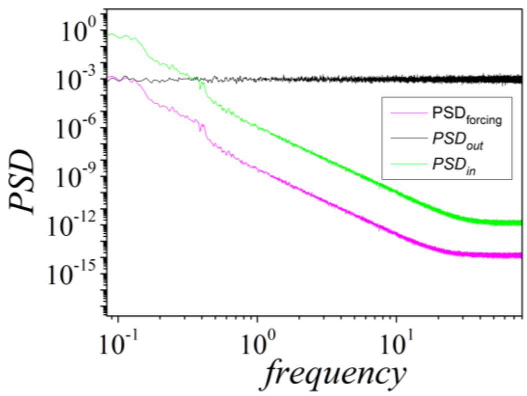

Figure 12. *PSD* for $\sigma^2 = 1$ and $f_0 = 1$.

Table 4. Efficiency, mechanical and electrical powers obtained with random excitation, Cases 9 to 20.

		Case 9	Case 10	Case 11	Case 12
f_0 \ σ^2		0.5	1	1.5	2
0.5	η	0.9659%	1.6066%	2.4287%	2.7173%
	P^m_{mec}	0.0313	0.06186	0.0856	0.1164
	P^m_{ele}	0.0003	0.0009	0.0020	0.0031
		Case 13	Case 14	Case 15	Case 16
1	η	2.7173%	2.5739%	2.1517%	1.8584%
	P^m_{mec}	0.1164	0.1637	0.3922	0.5016
	P^m_{ele}	0.0031	0.0053	0.0084	0.0093
		Case 17	Case 18	Case 19	Case 20
1.5	η	2.4152%	1.7368%	1.3872%	1.1597%
	P^m_{mec}	0.2782	0.5857	0.8530	1.1879
	P^m_{ele}	0.0067	0.0101	0.0118	0.0137

Table 5. PSD input, output and ratio *r* obtained with random excitation, Cases 9 to 20.

		Case 9	Case 10	Case 11	Case 12
f_0 \ σ^2		0.5	1	1.5	2
0.5	r	0.0062%	0.0204%	0.0445%	0.0785%
	PSD_{in}	47.8282	45.3620	43.8087	41.9907
	PSD_{out}	0.00299	0.0092	0.0195	0.0329
		Case 13	Case 14	Case 15	Case 16
1	r	0.0785%	0.1346%	0.1921%	0.1941%
	PSD_{in}	41.9907	40.5947	44.2293	45.0562
	PSD_{out}	0.0329	0.0546	0.0849	0.0874

		Case 17	Case 18	Case 19	Case 20
	r	0.1520%	0.2160%	0.2338%	0.2369%
1.5	PSD_{in}	42.1058	47.9937	52.7051	56.5229
	PSD_{out}	0.0639	0.1036	0.1232	0.1339

4 CONCLUSION

In this work, a numerical analysis of a piezomagnetoelastic system with nonlinear characteristic is done subjected to two different forcing conditions, one periodic and one Gaussian withe noise. A qualitative analysis of the system dynamic behavior is also presented, in order to identify a periodic or chaotic behavior using the Poincaré section. The bifurcation diagram shows the qualitative change of the behavior of the system varying the forcing parameters. Two different approached for the analysis where used. The first use the mechanical and electrical powers input and output and a given measure of efficiency. The second approach uses the PSD of the tip displacement of the beam and the voltage harvested by the piezoelectric material. The two approaches presented give different interpretations of the energy harvested by the system.

ACKNOWLEDGEMENTS

The authors would like to thank the Brazilian Research Agencies CNPq and CAPES for the support.

REFERENCES

Anton, S.R., and Sodano, H.A. (2007). A review of power harvesting using piezoelectric materials (2003–2006). Smart Mater. Struct. *16*, R1.

Erturk, A., Hoffmann, J., and Inman, D.J. (2009). A piezomagnetoelastic structure for broadband vibration energy harvesting. Appl. Phys. Lett. *94*, 254102.

Kumar, P., Narayanan, S., Adhikari, S., and Friswell, M.I. (2014). Fokker–Planck equation analysis of randomly excited nonlinear energy harvester. J. Sound Vib. *333*, 2040–2053.

Lefeuvre, E., Badel, A., Richard, C., and Guyomar, D. (2007). Energy harvesting using piezoelectric materials: Case of random vibrations. J. Electroceramics *19*, 349–355.

Moon, F.C., and Holmes, P.J. (1979). A magnetoelastic strange attractor. J. Sound Vib. *65*, 275–296.

Newland, D.E. (2005). An Introduction to Random Vibrations, Spectral & Wavelet Analysis: Third Edition (Mineola, N.Y: Dover Publications).

De Paula, A.S., Inman, D.J., and Savi, M.A. (2015). Energy harvesting in a nonlinear piezomagnetoelastic beam subjected to random excitation. Mech. Syst. Signal Process. *54–55*, 405–416.

Ramlan, R., Brennan, M.J., Mace, B.R., and Kovacic, I. (2009). Potential benefits of a non-linear stiffness in an energy harvesting device. Nonlinear Dyn. *59*, 545–558.

Shahruz, S.M. (2007). Increasing the Efficiency of Energy Scavengers. ArXiv07084412 Nlin.

Tang, L., Yang, Y., and Soh, C.K. (2010). Toward Broadband Vibration-based Energy Harvesting. J. Intell. Mater. Syst. Struct. *21*, 1867–1897.